# The crystal structure of HIV-1 Nef protein bound to the Fyn kinase SH3 domain suggests a role for this complex in altered T cell receptor signaling

Stefan Arold, Peet Franken, Marie-Paule Strub, Francois Hoh, Serge Benichou, Richard Benarous, Christian Dumas

# The crystal structure of HIV-1 Nef protein bound to the Fyn kinase SH3 domain suggests a role for this complex in altered T cell receptor signaling

Stefan Arold[1†], Peet Franken[1†], Marie-Paule Strub[1], Francois Hoh[1], Serge Benichou[2], Richard Benarous[2] and Christian Dumas[1*]

**Background:** Human immunodeficiency virus (HIV) Nef protein accelerates virulent progression of acquired immunodeficiency syndrome (AIDS) by its interaction with specific cellular proteins involved in signal transduction and host cell activation. Nef has been shown to bind specifically to a subset of the Src family of kinases. The structures of free Nef and Nef bound to Src homology region 3 (SH3) domain are important for the elucidation of how the affinity and specificity for the Src kinase family SH3 domains are achieved, and also for the development of potential drugs and vaccines against AIDS.

**Results:** We have determined the crystal structures of the conserved core of HIV-1 Nef protein alone and in complex with the wild-type SH3 domain of the p59$^{fyn}$ protein tyrosine kinase (Fyn), at 3.0 Å resolution. Comparison of the bound and unbound Nef structures revealed that a proline-rich motif (Pro-x-x-Pro), which is implicated in SH3 binding, is partially disordered in the absence of the binding partner; this motif only fully adopts a left-handed polyproline type II helix conformation upon complex formation with the Fyn SH3 domain. In addition, the structures show how an arginine residue (Arg77) of Nef interacts with Asp100 of the so-called RT loop within the Fyn SH3 domain, and triggers a hydrogen-bond rearrangement which allows the loop to adapt to complement the Nef surface. The Arg96 residue of the Fyn SH3 domain is specifically accommodated in the same hydrophobic pocket of Nef as the isoleucine residue of a previously described Fyn SH3 (Arg96→Ile) mutant that binds to Nef with higher affinity than the wild type.

**Conclusions:** The three-dimensional structures support evidence that the Nef–Fyn complex forms *in vivo* and may have a crucial role in the T cell perturbating action of Nef by altering T cell receptor signaling. The structures of bound and unbound Nef reveal that the multivalency of SH3 binding may be achieved by a ligand induced flexibility in the RT loop. The structures suggest possible targets for the design of inhibitors which specifically block Nef–SH3 interactions.

Addresses: [1]Centre de Biochimie Structurale, UMR C9955 CNRS, U414 INSERM, Université Montpellier I, Faculté de Pharmacie, Avenue C. Flahault, F34060 Montpellier, France and [2]ICGM, INSERM U332, 24 Rue du Fg St Jacques, 75014 Paris, France.

*Corresponding author.
E-mail: dumas@cbs.univ-montp1.fr

†These authors contributed equally to this work.

**Key words:** crystal structure, Fyn protein tyrosine kinase, HIV-1, Nef protein, SH3 domain

Received: **10 July 1997**
Revisions requested: **5 August 1997**
Revisions received: **27 August 1997**
Accepted: **3 September 1997**

**Structure** 15 October 1997, **5**:1361–1372
http://biomednet.com/elecref/0969212600501361



## Introduction

Infection by human immunodeficiency virus HIV-1 is associated with quantitative and qualitative T cell alterations that severely weaken the host's immune defence system and finally cause acquired immunodeficiency syndrome (AIDS). The molecular basis for this immunosuppression remains undefined.

Encoded at the 3′-end of the genome, the *nef* gene [1] of primate immunodeficiency viruses HIV-1, HIV-2 and simian immunodeficiency virus (SIV) is an important determinant of virulence in experimental infection of adult monkeys and in human disease [2–6]. A *nef*-deleted mutant of SIV which does not cause disease in adult macaques has been successfully used as a vaccine against challenge with pathogenic viruses, but causes AIDS in neonatal animals [7,8]. The critical role of Nef in human infection by the HIV-1 virus was also supported by studies of long term nonprogressing subjects infected with attenuated virus strains manifesting deletions in the *nef* gene [9,10].

The Nef viral molecule is a 206 amino acid N-terminal myristoylated protein [1,11] of 27 kDa, found in the cytoplasm and predominantly associated with the plasma membrane. Nef is one of the first HIV proteins to be produced at high levels in infected cells and the most immunogenic of the regulatory proteins [2,3]. Several recent reports provide evidence that Nef is a virion-associated protein, specifically cleaved in the viral particle by the viral protease to form a stable core domain [12–15].

Currently, three putative functions can conceivably account for the effects of Nef: down-regulation of the surface expression of CD4 [16–18], the principal viral receptor in T cells, and of major histocompatibility complex (MHC) I molecules [19]; modulation of the T-cell activation status [6,20–22]; and enhancement of viral growth rate and infectivity [23–25]. The molecular mechanisms by which these actions are accomplished remain elusive. Promotion of viral growth and CD4 down-regulation are functionally and genetically independent [25–27]. A correlation between direct Nef–protein kinase association and increase in infectivity has been shown [26,28]. Nef was reported to bind to serine/threonine kinases [28–30] and to various members of the Src family of protein tyrosine kinases: Hck and Lyn [26,31], Lck [32,33] and Fyn [33].

All these Src kinases are intricately linked in signal transduction pathways that control growth and cellular architecture [34,35]. Both Src-related protein tyrosine kinases p59$^{fyn}$ (Fyn) and p56$^{lck}$ (Lck) are abundantly expressed in T lymphocytes and have been implicated in antigen-induced T-cell activation [36–39]. Fyn is associated with the T cell antigen receptor (TCR) and plays an important role in TCR-mediated signaling. Hck shows restricted tissue distribution with expression in haematopoietic cells from the monocyte/macrophage lineage.

A Pro-x-x-Pro motif, known as classical Src homology region 3 (SH3) domain binding consensus, is found to be strictly conserved in HIV Nef isolates [26,31]. The 60 residue SH3 domain is present in a number of signal transduction and cytoskeletal proteins [40]. Within Src family tyrosine kinase members, the SH3 domains have approximately 60% identical sequences and they mediate direct substrate recognition, regulate kinase activity and control subcellular localisation [34]. The PxxP binding motif of SH3 domains present in Nef plays a critical role in enhancing viral replication [26].

The SH3 domain of Hck was reported to bind to Nef with an approximately 100-fold higher affinity than to the Fyn SH3 domain [31]. A single amino acid substitution in the Fyn SH3 domain (Arg96→Ile, as found in Hck) restored the high affinity of the Hck SH3 domain [31]. The structure of the HIV-1 NL43 isolate (HIV-1$_{NL43}$) Nef$_{core}$ region complexed to the R96I 'Hck-like' mutant Fyn SH3 domain has been published recently [41]. The expression of Hck kinase, however, is restricted to myeloid cells [42,43]; the Hck–Nef interaction can therefore not account for signaling defects in T lymphocytes. This fact highlights the importance of further identification of cellular partners of Nef in HIV target cells. The Fyn protein tyrosine kinase is expressed in T cells and could potentially be one of the physiological targets of Nef in HIV-infected CD4$^+$ lymphocytes. We have initiated crystallographic studies in order to address this question.

Our structural studies of HIV-1$_{LAI}$ Nef (from the LAI isolate) have focused on the central core domain (residues 58–206). This stable domain contains the interaction site for SH3 domains and corresponds to the product of HIV-1 protease cleavage [14,15,44]. We report here the first crystal structure of the core domain of unliganded HIV-1$_{LAI}$ Nef$_{core}$. The overall fold of the unliganded Nef$_{core}$ molecule is very similar to the solution structure of unliganded HIV-1$_{BH10}$ Nef$_{\Delta 2\text{-}39,\Delta 159\text{-}173,T71R}$ protein [45,46]. In addition, we have solved the crystal structure of the HIV-1$_{LAI}$ Nef$_{core}$ in complex with the human wild-type Fyn SH3 domain at 3.0 Å resolution and compared it with the crystal structure of HIV-1$_{NL43}$ Nef$_{core}$ bound to the high affinity R96I mutant of the Fyn SH3 domain [41]. The polyproline region (residues 71–77) of the unliganded Nef$_{core}$ molecule is partially disordered in the crystal structure, suggesting the PxxP motif is intrinsically flexible without bound SH3 domain. The comparison of the Fyn SH3 domain in the free state [47] and in our complex reveals that Nef induces local rearrangements in the hydrogen-bond network that holds a loop of the SH3 domain (termed the RT loop) in a rigid conformation. We show that the arginine residue at position 96 in the wild-type SH3 domain of Fyn is specifically accommodated in the same hydrophobic pocket of Nef as Ile96 in the previously reported structure of the high-affinity mutant of Fyn SH3 [41]. The interface buried between adjacent Nef molecules in the crystals is relatively large, about 8% of the total accessible surface of each molecule, and may provide a structural basis for the oligomerization of Nef reported by several authors [41,46,48,49]. The data presented here supports the idea that the complex between Fyn kinase and Nef could be biologically relevant in HIV-infected T cells.

## Results and discussion

### Overall structure of the HIV-1$_{LAI}$ Nef$_{core}$

We describe here three independent Nef$_{core}$ molecules from two different crystal forms at 3.0 Å resolution: two unbound Nef molecules in hexagonal and cubic crystal forms (Nef-A and Nef-C, respectively; see Materials and methods section), and the SH3-liganded Nef molecule in hexagonal crystal form (Nef-B). The common overall structure of the core domain of HIV-1 Nef protein (residues 58–206, LAI isolate) (Figure 1) is essentially identical to the crystal structure of SH3-liganded Nef (residues 54–205) from the HIV-1 NL43 isolate [41] and to the solution structure of unbound Nef$_{\Delta 2\text{-}39,\Delta 159\text{-}173,T71R}$ from the HIV-1 BH10 isolate [45,46]. The core domain folds into an α/β structure with four antiparallel β strands (sequentially labelled βA, 126–129; βB, 134–137; βC, 142–148; and βD, 180–185) flanked by an asymmetric distribution of four α helices. Two antiparallel helices, αA (residues 81–93) and αB (residues 104–118), cluster together proximate to one face of the central β sheet. The left-handed polyproline type II (PPII) helix, in the N-terminal region

(residues 71–77) is packed against the C-terminal part of helix αB. As pointed out by Lee *et al.* [41], geometrical distortion of the central β sheet is due to the presence of two conserved proline residues in strands βB (Pro136) and βC (Pro147), and to the limited number of residues involved in hydrogen bonds between these two interior strands. The N-terminal region from residue 58 to the polyproline motif, and the loop (residues 149–178) connecting strands βC–βD are disordered and not visible in the electron-density map.

The structure of the liganded Nef-B molecule (hexagonal crystal form) can be superimposed on the unliganded Nef-A (hexagonal crystal form) and Nef-C (cubic crystal form) with an overall root mean square (rms) deviation in Cα coordinates of 0.59Å and 0.78 Å, respectively, indicating that Nef does not undergo drastic structural changes upon complex formation. The temperature factors of the residues in the unbound Nef-A and Nef-C structures show mostly the same pattern as the temperature factors of the liganded Nef-B structure.

### Polyproline II conformation in the unliganded Nef core

The most striking structural feature of the unliganded Nef core domain appears to be the partly disordered conformation of the polyproline region (residues 71–77). Both ligand-free Nef molecules (Nef-A and Nef-C) lack interpretable electron density for the N-terminal region (residues 58–73) including the PPII helix motif, whereas the polypeptide chain in the SH3-liganded form (Nef-B) could be traced up to residue 71. The second half of the polyproline region (residues 74–77) is anchored through hydrogen bonding to the Nef core domain (residues 118–121) and shows higher temperature factors (average B factors 52 $A^2$) in the unliganded Nef forms than in the liganded Nef-B molecule (average B factors 28 $A^2$). These results seem to support that the polyproline region is partially disordered without a binding partner, suggesting it is intrinsically flexible. This region containing the PxxP motif, therefore, is not presented for interaction with the SH3 domain in the preferred left-handed PPII helix conformation. It is the SH3 domain that restrains its flexibility and stabilizes the PPII helix conformation upon complex formation. These structural findings are compatible with backbone dynamics and internal mobility in this polyproline region of unliganded Nef as calculated from NMR data [46].

### Structure of the Nef–$Fyn_{wt}$ SH3 complex

The basic fold of the Fyn SH3 domain (residues 85–141; Figure 2a) is similar to that described for the various Fyn SH3 domains whose structures, in the presence or absence of a ligand peptide, have been reported using X-ray crystallography and NMR spectroscopy [47,50–52]. The Fyn SH3 domain shows the highly conserved SH3 topology consisting of a β barrel formed by two approximal orthogonal β sheets, each composed of three antiparallel β strands. The N-terminal part of the Fyn SH3 domain is disordered before residue 84. The three connecting loops between the β strands are assigned as the distal, n-src and RT loops [47,50]. The Cα coordinates of the $Fyn_{wt}$ SH3 domain complexed to Nef can be superimposed within 0.48 Å rms deviation to the X-ray structure of the unliganded Fyn SH3 domain (molecule A of PDB entry 1SHF) [47]. The relative orientation of the SH3 domain with respect to Nef (Figure 2 is identical to that described for the Nef–$Fyn_{R96I}$ SH3 complex [41]: Cα coordinates for 157 pairs can be superimposed within 0.65 Å rms deviation (complex 2 in PDB entry 1EFN).

Most of the Fyn SH3 residues implicated in $Nef_{core}$ binding (Figure 3; Table 1) are strictly conserved among the Src kinase members listed. The Nef–Fyn SH3 complex forms via hydrophobic interactions, hydrogen bonds and specific electrostatic interactions. The Nef polyproline region (residues 71–77; coloured in blue in Figure 2b) including residues Pro72 and Pro75, packs on to aromatic residues of the SH3 domain as described for SH3–peptide complexes [50–53]. Nef forms additional tertiary interactions (yellow surface on Nef; Figure 2b) involving residues Lys82, Ala83,

**Figure 1**

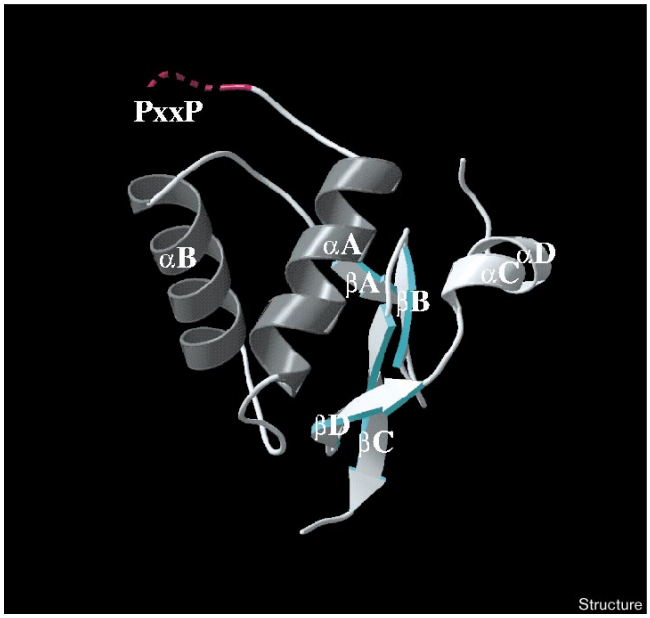


Ribbon diagram of the unliganded $Nef_{core}$ domain (residues 71–148 and 179–206). The polyproline type II helix is shown at the top of the figure in pink (residues 71–77) and is disordered before residue 74 (pink dotted line). This helix is followed by two antiparallel α helices (αA and αB) and a layer of four β strands (βA–βD) with a disordered loop connecting strands βC and βD (residues 149–178, not visible in the crystal structure). Finally, there are two short α helices (αC and αD) at the C terminus. (The figure was created with the programs MOLSCRIPT [71] and RASTER3D [72].)

**Figure 2**

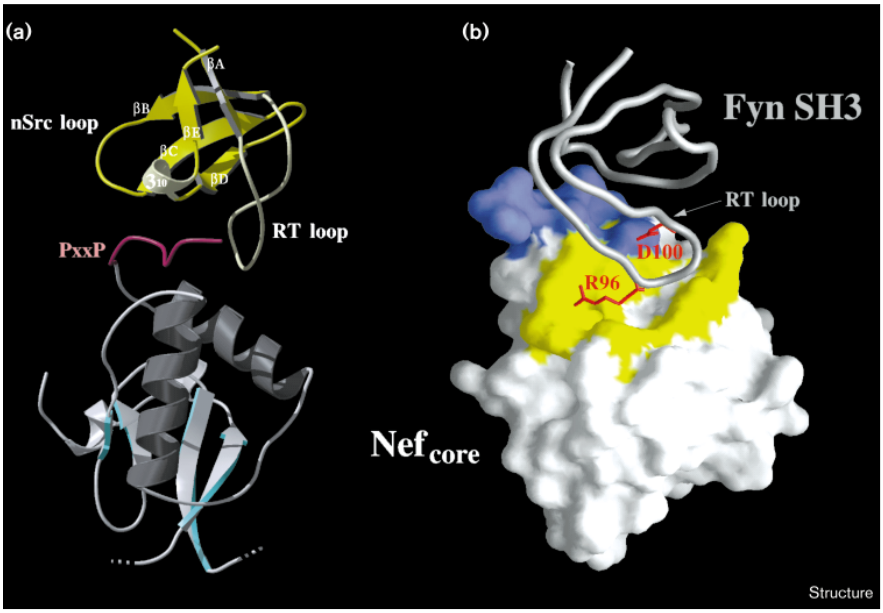


Structure of the HIV-1 $Nef_{core}$–$Fyn_{wt}$ SH3 complex. **(a)** Ribbon drawing of the $Nef_{core}$ domain complexed to the $Fyn_{wt}$ SH3 domain. The wild-type Fyn SH3 domain is shown at the top in yellow and comprises a β barrel consisting of five antiparallel β strands which form two perpendicular β sheets. The polyproline type II helix of Nef is shown in pink. The limits of the disordered loop region (residues 149–177) are indicated by dotted lines. (The figure was prepared using MOLSCRIPT [71] and RASTER3D [72].) **(b)** Molecular surface representation of the HIV-1 $Nef_{core}$ domain and the Fyn SH3 backbone worm (grey). The views in (a) and (b) are approximately orthogonal. The Nef surface representation shows the polyproline type II helix (residues 71–77) in blue and the other residues involved in binding of the Fyn SH3 domain (K82, A83, D86, L87, F90, W113, T117, Q118 and Y120 ) in yellow. Arg96 and Asp100, critical residues within the RT loop of the Fyn SH3 domain are shown in red. (The figure was produced using GRASP [73].)

Asp86, Leu87 and Phe90 of the αA helix residues Trp113, Thr117 and Glu118 of the αB helix and Tyr120 of the loop connecting the αB helix to strand βA. Regarding Fyn, most residues in contact with Nef and all those which form the specificity determinating bounds with non-PxxP residues of Nef, are situated in the RT loop (Figures 2b and 3). At least, three distinct regions on the surface of the Fyn SH3 domain are involved in the Nef interface. Most of these regions are conserved in other Src family kinases: a predominant aromatic cluster comprising residues Tyr91 and Tyr93 (labels a and b in Figure 3) followed by residues 97–100 (labels c to g) which map in the middle of the RT loop: the conserved Trp119 residue (label h); and the Pro-x-Asn-Tyr motif in the $3_{10}$-helix region (labels i, j and k).

The accessible surface areas of the isolated $Nef_{core}$ and $Fyn_{wt}$ SH3 domain are 6430 Å$^2$ and 3760 Å$^2$, respectively. As a result of complex formation, some of the surface area is buried in the interface between both molecules. The total buried surface area involved in the interface represents 1270 Å$^2$, with 630 Å$^2$ and 640 Å$^2$ for SH3 and Nef, respectively. All these values are within the usual range for protein complexes and comparable to those described for the $Nef_{core}$–$Fyn_{R96I}$ SH3 complex [41]. The values obtained for the buried surface area establish that the interacting surface of Nef can be sufficiently large to form a stable complex with the $Fyn_{wt}$ SH3 domain. The contribution of each residue to the buried solvent-accessible surface is shown in Figure 4. In the $Nef_{core}$ domain, the most important contribution to the interface area comes

**Figure 3**

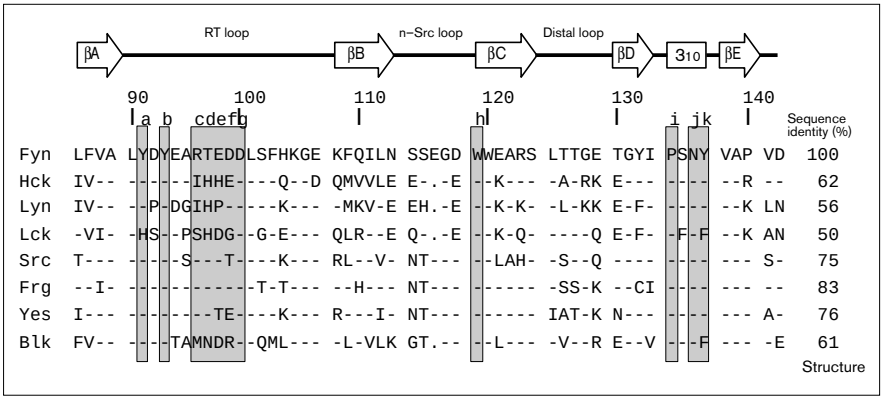


Assignment of secondary structure elements of the Fyn SH3 domain and alignment of the known human amino acid sequences of the Src protein tyrosine kinase family. Fyn SH3 residues involved in the Nef–SH3 interface (letters a–k), and homologous aligned residues, are enclosed in shaded boxes. Strictly conserved residues implicated in Nef core binding are labelled b, g, h, i and j (see text for details). The amino acid numbering corresponds to $p59^{fyn}$.

**Table 1**

**Residues involved in the HIV-$1_{LAI}$ Nef–$Fyn_{wt}$ SH3 interaction.**

| | Fyn | | Nef | Interactions |
|---|---|---|---|---|
| | Label | Residue | | |
| RT loop | a | Y91 | **P72** | Hydrophobic |
| | b | Y93 | **V74** | Hydrophobic |
| | c | R96 | F90, W113, I114 | Hydrophobic |
| | | | T117 | Hydrogen bond R96 NH2 to T117 Oγ1 |
| | d | T97 | Y120 | Hydrogen bond T97 Oγ1 to Y120 OH |
| | e | E98 | D86 | Hydrogen bond E98 N to D86 Oδ1 |
| | f | D99 | K82 | Salt bridge |
| | g | D100 | **R77** | Salt bridge |
| β Strand C | h | W119 | **P75** | Hydrogen bond W119 Nε1 to P75 O |
| | | | **V74**, **R77** | Hydrophobic |
| $3_{10}$ Helix | i | P134 | **P75** | Hydrophobic |
| | j | N136 | **Q73** | Hydrogen bond N136 Nδ2 to Q73 O |
| | k | Y137 | **P72** | Hydrogen bond Y137 OH to P72 O |
| | | | **V74** | Hydrophobic |

The SH3 labels a to k correspond to the convention of Figure 3. Nef residues of the polyproline region are indicated in bold letters. A distance cut-off of 3.6 Å was used for possible hydrogen bonds; for hydrophobic interactions, a distance cut-off of 4.0 Å was used.

from residues Pro72, Val74, Pro75, Arg77 of the PPII helix and Asp86 of helix αA. The residues of the Fyn SH3 domain that make the largest contributions to the buried solvent-accessible area are Arg96 and Trp119, providing 160 $Å^2$ and 100 $Å^2$, respectively. All the calculations of buried surface utilized a 1.4 Å probe radius.

### Nef induces a conformational change in the Fyn SH3 RT loop

Flexibility in protein surface loops plays an important role in molecular recognition. Conformational gating can provide a mechanism to increase ligand specificity by 'induced fit'. In the unbound Fyn SH3 domain [47,52], the conformation of the RT loop (residues 90–108) is stabilized in a rigid conformation by a hydrogen-bonding network (Figure 5a). An important component of this hydrogen-bond network is the Asp100 residue. As illustrated in Figure 5a, Asp100 plays a pivotal role: its carboxylate group positioned in the centre of the RT loop serves to anchor the sidechains of Tyr93 and Thr97 as well as the mainchain of Thr97 and Arg96 through five hydrogen bonds. The stabilized RT loop is fixed by two additional hydrogen bonds to residue Tyr132 of the underlying strand βD.

**Figure 4**

Loss of solvent-accessible surface area of the sidechain residues involved in the Nef–$Fyn_{wt}$ SH3 interface. Solvent accessibilities were calculated with a rolling sphere of radius 1.4 Å.

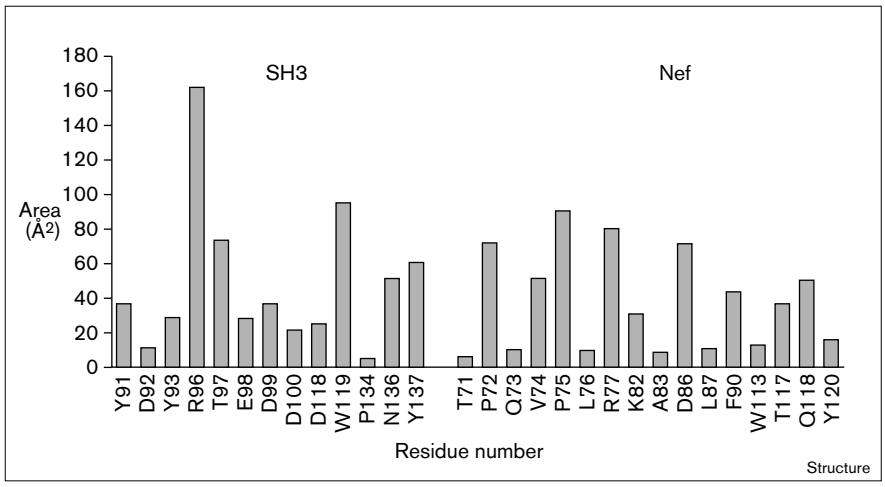

**Figure 5**

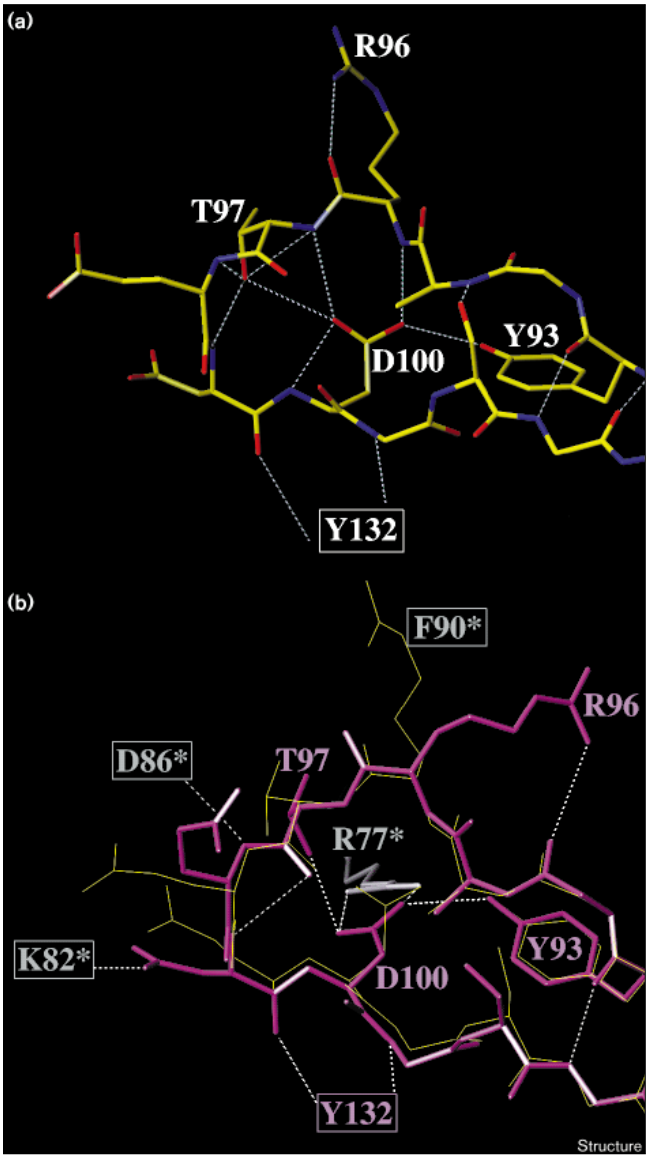


Conformational rearrangement in the Fyn SH3 RT loop upon binding to the $Nef_{core}$ domain. **(a)** The RT loop region of unliganded Fyn SH3 (PDB entry 1SHF) [46] in stick representation. Atoms are coloured by type: C, yellow; N, blue; O, red. Asp100 plays a pivotal role in maintaining a network of hydrogen bonds (indicated by dashed lines). The RT loop is fixed to Tyr132 of the underlying β strand. **(b)** Superimposition of the RT loop region of the unliganded (yellow) and liganded (pink) Fyn SH3 domain, shown as an all-atom stick figure. Sidechains of residues not involved in binding are omitted for clarity; Nef residues are indicated by an asterisk. Residues not represented in the figure are shown boxed. Large displacements were observed for Fyn residues Arg96 and Asp100, which forms a salt bridge to $Nef_{core}$ Arg77.

The strictly conserved residue Arg77 in the P-3 position [31] of the Nef polyproline region plays a key role in the Nef–SH3 interfacial electrostatic interaction. Arg77 is anchored to the $Nef_{core}$ domain via hydrogen bonds to the mainchain atoms of residues 118, 119 and 120. In the absence of a ligand, Arg77 already partially locks residues 75–77 in a PPII helix conformation and is held in an optimal position for interaction with SH3 domains. Upon binding to the Fyn SH3 domain, Arg77 reaches out for Fyn SH3 Asp100 and bends it away from its central position in the RT loop by the formation of a salt bridge (Figure 5b). Similar ion pairing interactions have been described in SH3–peptide complexes [50–53]. The displacement of Asp100 results in the disruption of all of its three hydrogen bonds to mainchain nitrogens (Figure 5b). This loss of the stabilizing hydrogen bonds renders the stretch of residues 95–101 of the RT loop floppy enough to adapt to the Nef surface. In particular, this flexibility enables the large displacement of Arg96 (1.4 Å displacement for the Cα atom, and 8 Å for the guanidinium group), that is necessary to stack its aliphatic moiety onto the Phe90 residue which is localized in a crevice on the surface of Nef. This mechanism of introduced flexibility may provide an explanation for the ability of the Nef protein to bind to different SH3 target molecules.

### Hot spots of binding energy in the Nef–SH3 interface

Tertiary interactions seem to be a common mechanism by which relevant levels of specificity are achieved. Nef forms a high-affinity complex with the $Fyn_{R96I}$ SH3 domain ($K_D$ = 380 nM) whereas a lower affinity ($K_D$ > 20 μM) was reported for wild-type Fyn SH3 [26,31]. The superimposition of the Nef–$Fyn_{wt}$ SH3 structure with the structure of Lee *et al.* [41] (Figure 6), shows that Arg96 mimics Ile96 of the R96I mutant Fyn SH3 domain. In a similar manner to Ile96, Arg96 presents its aliphatic moiety to the Nef hydrophobic cavity comprising residues Leu87, Phe90 and Trp113. The Nη1 atom of the Arg96 guanidino group replaces a bound water molecule in the model of Nef–$Fyn_{R96I}$ SH3 [41]. The Ile96 sidechain and polymethylene chain of Arg96 are fully buried at the interface, but the charged guanidinium group of Arg96 is partially exposed to the solvent (25 $Å^2$ of solvent accessible surface). An acidic residue in the vicinity of Arg96 (SH3 Glu94) contributes to electrostatic complementarity. Thus, the complex between Nef and the wild-type SH3 domain of Fyn reveals that the sidechain of Arg96 fits into the hydrophobic pocket of Nef as does Ile96 of the Fyn SH3 mutant, and does not seem to result in an energetically unfavourable situation. The reported loss in binding free energy of about 2.3 kcal $mol^{-1}$ for the wild-type SH3 domain cannot be explained by the structure alone and may result from partial desolvation and entropic penalties due to the rearrangement of the Arg96 sidechain.

The above mentioned Asp100 residue of the SH3 domain and Arg77 residue of Nef are strictly conserved in both molecules and engage in the formation of a salt bridge. This electrostatic interaction is a prominent feature of peptide–SH3 interactions [50–53], and may constitute a

**Figure 6**

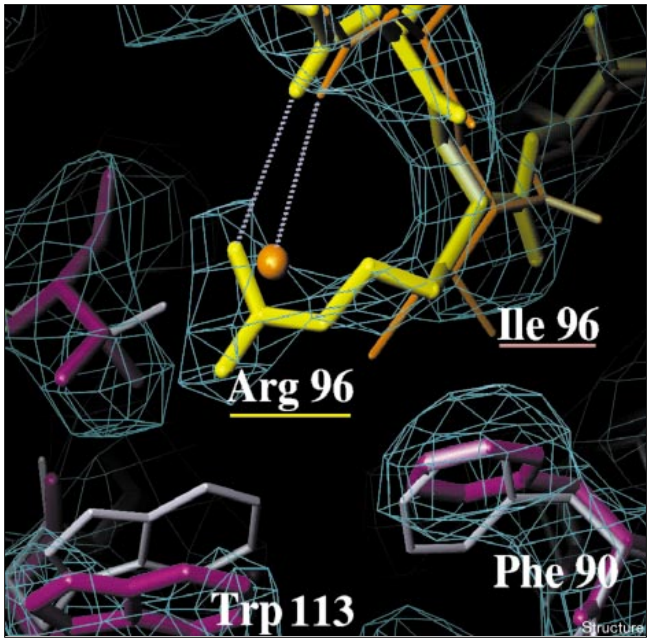


Arg96 of $Fyn_{wt}$ SH3 domain in its simulated annealing ($2F_o–F_c$) electron density omit map [63] contoured at 1.1σ. The residues of the wild-type Fyn SH3 (yellow) and HIV-$1_{LAI}$ Nef (purple) are superimposed onto $Fyn_{R96I}$ SH3 (orange) and HIV-$1_{NL43}$ Nef (grey; PDB entry 1EFN) [41]. Hydrogen bonds are drawn as dashed lines. A water molecule hydrogen bonded to HIV-$1_{NL43}$ Nef is represented by an orange CPK sphere.

second 'hot spot' of binding energy. In the present structure, Nef Arg77 is stacked against the Nef Trp119 sidechain. The molecular surfaces of these residues are largely buried upon complex formation (Figure 4), indicating an additional key contribution to the hydrophobic core of the functional epitope. The electrostatic interaction between Nef Arg77 and SH3 Asp100 in the RT loop also serves to position the SH3 Arg96 sidechain inside the hydrophobic crevice on the surface of Nef. Further evidence regarding the importance of these residues has been provided by biochemical and mutational experiments describing altered SH3 binding affinity as a result of the substitution of these residues [54].

A precise evaluation of the contribution of these residues to the stability of the complex would require high-resolution structure determination for both liganded and unliganded Nef molecules, and thermodynamic measurements.

### Sequence variability in the polyproline region of Nef

Sequence comparison of various Nef isolates shows that the core domain of Nef (excluding the disordered βC–βD) is well conserved [15,41]. Most of the strictly conserved positions in the $Nef_{core}$ domain are clearly implicated either in stabilizing the hydrophobic core or binding the SH3 domain [41]. The LAI strain used in this paper has a threonine residue at position 71. Unlike this laboratory adaptated HIV-1 strain, almost all *nef* alleles isolated directly from patients encode an arginine or a lysine at position 71 rather than a threonine [55,56]. As shown in Figure 7, the threonine sidechain does not form any major contacts with the SH3 domain in the proximity of Tyr137. In contrast, the Arg71 residue in the crystal structure of Lee *et al.* [41] enhances the stability of the complex by forming a hydrogen bond with the hydroxyl group of Tyr137 and electrostatic interactions with acidic residues Asp92 and Glu94 of Fyn SH3 (Figure 7). In the Lee *et al.* structure, mainchain atoms of Arg71 and Pro72 in Nef, as well as Tyr91 in the SH3 domain, are significantly displaced (about 0.9 Å) relative to the position in our complex. These observations are compatible with the results of previous studies showing significantly increased binding affinity of Lyn and Hck SH3 to the $Nef_{T71R}$ mutant [26]. The gain in affinity for the Arg71 strains may

**Figure 7**

Superimposition of the crystal structures of Nef–SH3 complexes. Stereoview of the interface showing the environment of the Nef polyproline type II helix region (residues 71–77) and conserved residues. The two Nef isolates are superimposed: Nef HIV-$1_{LAI}$ isolate in green and $Nef_{T71R}$ HIV-$1_{NL43}$ isolate (Nef-D molecule in PDB entry 1EFN) in red. The hydrogen bond between the Arg71 sidechain and Tyr137 of $Fyn_{R96I}$ is shown as a dotted white line. The SH3 domains are coloured in light purple and dark purple for $Fyn_{wt}$ and $Fyn_{R96I}$ (SH3-C molecule in PDB entry 1EFN), respectively. (Figure generated using the program O [69].)

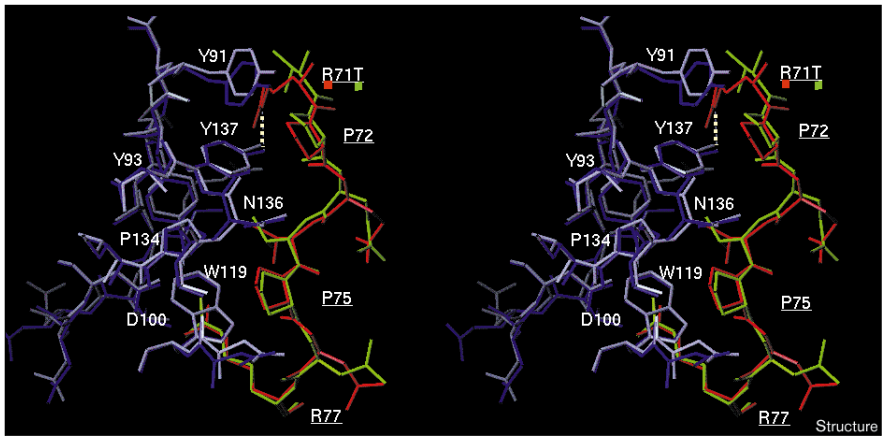

explain why in many isolates mutational pressure is directed from threonine to arginine or lysine.

### Crystal packing and the oligomeric structure of HIV-1 Nef

The interface between adjacent $Nef_{core}$ molecules in both crystal forms is large (~8% of the total surface) and may be interpreted as Nef forming dimers and trimers, for the hexagonal and cubic crystal forms, respectively. In the hexagonal crystal form, the contact formed between Nef molecules related by the local axis involves residues located in the αB helix and the αB–βA loop. The majority of the contacts are made by hydrophobic residues: Ile109, Leu112, Tyr115 and Phe121. Most of these residues are conserved among HIV-1 Nef isolates. The association of the two Nef molecules buries a surface area of 900 Å$^2$. In the more densely packed P23 crystal, the trimer interface of the unliganded Nef covers 1680 Å$^2$ of the solvent-accessible surface (i.e. ~9% of the monomer surface). Moreover, oligomer formation will be favoured in the intact cell because the myristoylated Nef molecules are tethered to the membrane. The above described packing contacts for $Nef_{core}$ domains may be either crystal artefacts, or correspond to 'crystal oligomers' [57] which may have formed in solution before crystallization. Additional evidence for the formation of Nef dimers, trimers and oligomers has been reported previously [48,49] and it has been suggested that these multimers may have a biological function. Nevertheless, the cellular role, if any, of Nef oligomerization remains to be determined.

The asymmetric unit of the Nef–Fyn SH3 cocrystals contains two $Nef_{core}$ molecules and one SH3 domain (i.e. one Nef–SH3 complex and a free Nef molecule). This crystal packing is characterized by a high solvent content (70%). It is very likely that the disordered additional 16 N-terminal residues of our Fyn construction sterically hinder the inclusion of the second SH3 domain. Furthermore, the stoichiometry of Nef:Fyn SH3 mixture was adjusted to 1.3:1 for optimal crystal growth. Although rarely observed, a similar packing constraint was described for the p53 tumor suppressor–DNA complex [58], where both one free and two DNA-liganded p53 molecules were present in the asymmetric unit.

### Functional implications of the Nef–Fyn kinase interaction in T cells

The Src family protein tyrosine kinase, Fyn, is expressed in T cells and is crucially involved in the initiation of TCR signal transduction [34,35]. Several studies support the importance of a functional association of Fyn with TCR machinery. The mechanisms by which Fyn regulates TCR/CD3 signaling, however, are still not completely understood. Many cellular proteins associate with Fyn in T cells, including ZAP-70 [59], CD43 [60] and Fas protein [61]. Fyn has specific targets which are rapidly phosphorylated at tyrosine residues following TCR stimulation [62]. Recent genetic and biochemical studies [20] have shown that Nef blocks a receptor-proximal event in the TCR/CD3 pathway, and that this effect is mediated by the interaction of Nef with a specific SH3 domain present in the TCR complex. Combined with these experiments, our structural data support the identification of Fyn SH3 as the candidate target of Nef in T cells and strengthen the hypothesis that the complex of Nef with the wild-type Fyn kinase forms *in vivo*. Aberrant TCR-mediated signaling may involve dysfunctional regulation of Fyn by Nef. The Src family kinases share common structural features and regulation. The recent observation that Nef can stimulate Hck kinase *in vitro* [63] suggests that Nef–SH3 interaction can destabilize the repressed conformation of Hck [64]. This SH3-dependent activation of Src kinases may be a general property of Nef.

The interaction of Nef with the TCR machinery is likely to be critical for AIDS pathogenesis. The resulting alteration in the T-cell activation status and perturbations in TCR-mediated signaling may lead to an increase in virus production and contribute to the immune unresponsiveness of infected T cells.

## Biological implications

**The *nef* gene of human immunodeficiency virus (HIV) and simian immunodeficiency virus (SIV) encodes a 27 to 34 kDa myristoylated protein. Expression of the HIV Nef protein has been linked to both decreased cell surface expression of CD4, the principal HIV receptor in T cells, and an impairment of signal transduction in these infected cells. Moreover, the *nef* gene is required for the induction of AIDS. Immunization of adult macaques with live attenuated SIV lacking the *nef* gene has been shown to protect against challenge with full-length pathogenic SIV. It is clear, therefore, that Nef protein plays a key role in human infection by HIV.**

**A proline-rich motif (Pro-x-x-Pro) has been found to be strictly conserved in all Nef proteins from HIV and SIV isolates. These PxxP motifs are recognized by Src homology 3 (SH3) signaling domains, and Nef has been shown to bind to a subset of SH3 domains from members of the Src family of protein tyrosine kinases. The Fyn tyrosine protein kinase is expressed in T cells and has been proposed as one of the physiological targets for Nef in infected cells. The results reported in this study have gone some way towards addressing this question.**

**The crystal structures of unliganded and Fyn SH3-bound Nef core molecules provide new insights into the mode of action of Nef, as well as delineating the structural features, in both the viral protein and the SH3 domain, which govern the specificity and potency of this interaction. The N-terminal region of the Nef core domain containing the PxxP motif is partially disordered**

**in the absence of bound ligand, and only fully adopts a left-handed polyproline type II helix conformation upon binding to the SH3 domain. Nef interacts with the SH3 domains of the Hck and Fyn protein kinases in structurally similar yet energetically distinct manners. Hck is not expressed in T cells and its association with Nef therefore cannot account for the signaling defects observed in these cells. The reported structures provide evidence that the Nef–Fyn kinase complex forms *in vivo*: both proteins coexist in HIV-infected T cells and are targeted to the membrane by myristoylation; and the Nef surface that interacts with the Fyn SH3 domain is highly conserved across HIV-1 isolates. The Fyn protein kinase is critical in T-cell receptor (TCR)-mediated activation of T cells. The direct interaction between Nef and Fyn could partially explain the alteration in the T-cell activation status and aberrant TCR-mediated signaling which are observed in HIV-infected T lymphocytes.**

**Molecules which block specific Nef–Fyn SH3 contacts could prove to be useful therapeutic agents. In addition, the identification of HIV peptide epitopes is essential for AIDS vaccine development and this is of particular importance for Nef, which is one of the most immunogenic HIV proteins. The structural data reported here provide further useful information for the future structure-based drug design of specific inhibitors and the development of an optimal vaccine strategy.**

## Materials and methods

*Crystallization and data collection*

The HIV-$1_{LAI}$ $Nef_{core}$ domain (residues 58–206) and Fyn SH3 domain (residues 72–142) were expressed in *Escherichia coli* as glutathione S-transferase fusion proteins. A detailed account of protein preparation, purification and crystallization will be given elsewhere (PF *et al.,* unpublished data). Two crystal forms were used for structure determination. Firstly, unliganded HIV-1 Nef formed cubic crystals belonging to space group P23 (a = b = c = 86.4 Å); a single Nef molecule was present per asymmetric unit. A selenomethionyl version of the protein was purified and crystallized under conditions identical to those for the native unliganded protein. Two additional mercury heavy-atom derivatives were prepared by controlled soaking. Secondly, Nef cocrystallized with $Fyn_{wt}$ SH3 formed hexagonal crystals that grew in space group $P6_522$ (a = b = 108.2 Å, c = 223.7 Å). Data for the cubic and the hexagonal crystal forms were collected to 3.0 Å resolution at the ESRF synchrotron radiation source (Beamline D2AM, Grenoble, France) on CCD detector at $\lambda = 1.0373$ Å and $\lambda = 0.9783$ Å (native 1 and derivatives; Table 2). The data collection was performed on flash frozen crystals except for native 1 and heavy-atom derivatives of the cubic crystal form (Table 2). The X-ray diffraction images were processed by the program XDS [65] adapted for the D2AM beamline. Structure factor analysis were carried out with the CCP4 suite [66].

*Structure determination*

Both multiple isomorphous replacement (MIRAS) and molecular replacement (MR) methods were used to solve the structure of unbound Nef cubic crystals. Refinement of heavy-atom parameters and phase-angle calculations (Table 2) were performed with the program MLPHARE (CCP4). MIRAS phases gave a mean overall figure of merit of 0.43 at 3.1 Å and were significantly improved by the process of solvent flattening and histogram matching as implemented in the program DM (CCP4). The electron-density map with a 3.1 Å resolution limit, however, was poor. Several secondary structure elements (two β strands and two α helices) were identifiable and could be built in the idealized map. They were confirmed by the MR solution. An anomalous Fourier map gave one peak corresponding to selenium in residue Met79. MR was performed with the AMoRe program [67] starting from the the structure of HIV-$1_{NL43}$ $Nef_{core}$ [41] (PDB entry 1EFN) as a search model. A single clear solution gave an $R_{factor}$ of 39% and a correlation coefficient of 0.67 within the range of 8 Å to 3.2 Å, whereas the next solution had an $R_{factor}$ of 55% and a correlation coefficient of 0.29. Model and MIRAS phases were combined at the beginning of refinement in order to minimize the bias from the initial model.

The structure of the HIV-$1_{LAI}$ Nef–$Fyn_{wt}$ SH3 complex was determined by MR using the AMoRe program [67]. The crystal structures of Fyn SH3 [47] (SH3-B molecule in PDB entry 1SHF) and HIV-$1_{NL43}$ $Nef_{core}$ [41] (PDB entry 1EFN) were used as molecular templates. Both enantiomeric space groups $P6_122$ and $P6_522$ were tried in MR runs.

**Table 2**

**Data collection and phasing statistics.**

| | Unliganded Nef | | | | | Nef–SH3 complex |
|---|---|---|---|---|---|---|
| | Native 1 | SeMet | HgAc | PCMB | Cryo | |
| Diffraction limit (Å) | 3.1 | 3.5 | 3.4 | 3.1 | 3.0 | 3.0 |
| No. unique reflections | 3812 | 2472 | 2786 | 3731 | 3998 | 14 778 |
| Observations | 18 555 | 12 587 | 11 333 | 15 489 | 20 384 | 57 175 |
| Completeness (%) | 93 | 86 | 89 | 91 | 92 | 91 |
| $R_{sym}$ (%)* | 7.2 | 7.1 | 7.8 | 6.8 | 6.6 | 6.7 |
| $R_{deriv}$ (%)† | – | 14.5 | 21.4 | 23.2 | | |
| Phasing power‡ | – | 1.2 | 0.9 | 0.8 | | |
| Space group | P23, a = b = c = 86.4 Å | | | | | $P6_522$, a = b = 108.2 Å c = 223.7 Å |
| Asymmetric unit content | Z = 1 with Vm = 3.1 $Å^3$/Da | | | | | Z = 1, 1 SH3/2 Nef, Vm = 4.2 $Å^3$/Da |

*$R_{sym} = \Sigma \Sigma_i | I_i - \langle I \rangle | / \Sigma \langle I \rangle$, where $I_i$ are the intensity measurements for a reflection and $\langle I \rangle$ is the mean value for this reflection. †$R_{deriv} = \Sigma | F_{PH} - F_P | / \Sigma F_P$, where $F_{PH}$ and $F_P$ represent the structure-factor amplitude of the derivative and native crystals, respectively. ‡Phasing power = root mean square $f_H/E$, where $f_H$ = the mean calculated heavy-atom structure-factor amplitude and E = the residual lack of closure error.

**Table 3**

**Refinement statistics.**

| | Nef cubic P23 | Nef hexagonal $P6_522$ |
|---|---|---|
| Resolution range (Å) | 30–3.0 | 30–3.0 |
| Unique reflections ($F > 2\sigma F$) | 3800 | 11 662 |
| Number of nonhydrogen atoms | 895 | 2216 (857/463/896)§ |
| Final R factor (%)* | 22.4 | 22.2 |
| Free R factor (%)† | 28.1 | 28.2 |
| Average B factors (Å²) | 38 | 33.5 (32.9/32.4/36.5)# |
| Rms deviation from ideality‡ | | |
| bonds lengths (Å) | 0.009 | 0.010 |
| bond angles (°) | 1.9 | 1.4 |
| dihedral angles (°) | 23.7 | 24.1 |
| Ramachandran plot quality | | |
| residues in core regions (%) | 81 | 83 |
| residues in disallowed regions | 0 | 0 |

*R factor $= \Sigma ||F_o| - |F_c|| / \Sigma |F_o|$, where $F_o$ and $F_c$ represent the observed and calculated structure factors, respectively. †Free R factor computed for 10% of the data chosen randomly. ‡Calculated by X-PLOR. §Number of nonhydrogen atoms (NefA, NefB and SH3 domain in hexagonal crystal form). #Average B factors for NefA, NefB and the SH3 domain in the hexagonal crystal form.

Despite an extensive search, clear solutions were detected in space group $P6_522$ for two Nef molecules but only for one Fyn SH3 molecule. Following rigid-body refinement using the AMoRe program, the correct solution for the three molecules had a correlation coefficient of 0.60 and an $R_{factor}$ of 35.7% within the range of 12 Å to 3.5 Å. Consistent results were obtained using various resolution ranges. All positions proposed by AMoRE for the second SH3 molecule were incorrect in terms of crystal packing and did not lead to a significantly higher correlation. The unliganded Nef molecule (Nef-A) and SH3-bound Nef molecule (Nef-B) are related by an approximate local twofold axis that is 0.4° off 180° rotation and 0.3 Å off zero translation.

### *Model building and refinement*

The unliganded Nef model in the cubic crystal form (Nef-C) was refined by several rounds of molecular dynamics and energy minimization with X-PLOR [68] against the native 2 data set (Table 2), followed by manual rebuilding. Group temperature-factor refinement was carried out for each residue. The present model consists of 895 nonhydrogen atoms. No solvent molecules were added to the structure. The N-terminal residues 58–74 and residues 148–178, that belong to a mobile loop, could not be traced in the current electron-density maps. The final R factor of the refined model is 22.4% ($R_{free}$ = 28.1%) and the stereochemistry is reasonable (Table 3).

The MR model for the complex Nef–Fyn SH3 in the hexagonal crystal form consisted of two $Nef_{core}$ molecules and only one Fyn SH3 domain. The expected second SH3 domain could not be retrieved by noncrystallographic symmetry (NCS) electron-density averaging. Close examination in the final refinement cycles of the electron-density maps using $2F_o–F_c$ and $F_o–F_c$ coefficients, did not reveal any significant residual density. NCS restraints on both Nef molecules, except for the polyproline region (residues 71–77), were kept throughout the refinement and only released at the final step. The final model comprises one complex, the Fyn SH3 domain (residues 85–141) bound to a Nef-B molecule (residues 71–148 and 178–203), and one single unliganded Nef molecule (Nef-A, residues 74–147 and 179–203). After extensive refinement, some strong residual density was found in the crevice between the two Nef molecules of the asymmetric unit. As Nef–Fyn cocrystal formation depends crucially on the presence of β-octyl α-D-glucoside, this density is likely to represent this detergent molecule and was modelled accordingly. The glucose moiety of this detergent molecule is confined in a hydrophilic environment formed by the residues Asp108, Gln104, Asp111 and Asn126, whereas the lipid tail is partially disordered. This same cavity was seen to bind a trimethyl lead ion in the $Fyn_{R96I}$–$Nef_{core}$ [41] structure. Refinement statistics are given in Table 3.

The program O [69] was used for model building and graphical display of the molecules and electron-density maps. The stereochemistry of the models was monitored with the program PROCHECK [70].

### *Accession numbers*

The coordinates for the free Nef and Nef–$Fyn_{wt}$ SH3 structures have been deposited in the Protein Data Bank with accession codes 1avv and 1avz, respectively.

## Acknowledgements

The work was supported by CNRS, INSERM, Fondation pour la Recherche Médicale (FRM Sidaction) and Agence Nationale pour la Recherche sur le SIDA (ANRS). PF is a Postdoctoral fellow of FRM Sidaction and SA a doctoral fellow of Ministére de l'Enseignement Supérieur et de la Recherche. We are grateful to J Kuriyan, CH Lee and S Grzesiek for the use of the Nef coordinates and to S Roche for providing the SH3 Fyn expression plasmid. We thank J M Lhoste for continuous support of the project and helpful discussions, M Roth, E Fanchon and R Kahn for their help using the D2AM ESRF beam line and J Janin, S Roche and A Padilla for the critical reading of this manuscript.

## References

1. Allan, J.S., *et al.*, & Essex, M. (1985). A new HTLV-III/LAV encoded antigen detected by antibodies from AIDS patients. *Science* **230**, 810–813.
2. Trono, D. (1995). HIV accessory proteins: leading roles for the supporting cast. *Cell* **82**, 189–192.
3. Littman, D.R. (1994). Immunodeficiency viruses. Not enough sans Nef. *Curr. Biol.* **4**, 618–620.
4. Cullen, B.R. (1994). The role of Nef in the replication cycle of the human and simian immunodeficiency viruses. *Virology* **205**, 1–6.
5. Kestler, H.W., *et al.*, & Desrosiers, R.C. (1991). Importance of the *nef* gene for maintenance of high virus loads and for development of AIDS. *Cell* **65**, 651–662.
6. Du, Z., *et al.*, & Desrosiers, R.C. (1995). Identification of a *nef* allele that causes lymphocyte activation and acute disease in macaque monkeys. *Cell* **82**, 665–674.
7. Baba, T.W., *et al.*, & Ruprecht, R.M. (1995). Pathogenicity of live attenuated SIV after mucosal infection of neonatal macaques. *Science* **267**, 1820–1825.
8. Daniel, M.D., Kirchhoff, F., Czajak, S.C., Sehgal, P.K. & Desrosiers, R.C. (1992). Protective effects of a live attenuated SIV vaccine with a deletion in the *nef* gene. *Science* **258**, 1938–1941.
9. Kirchhoff, F., Greenough, T.C., Brettler, D.B., Sullivan, J.L. & Desrosiers, R.C. (1995). Brief report: absence of intact *nef* sequences in a long-term survivor with nonprogressive HIV-1 infection. *N. Engl. J. Med.* **332**, 228–232.
10. Deacon, N.J., *et al.*, & Mills, J. (1995). Genomic structure of an attenuated quasi species of HIV-1 from a blood transfusion donor and recipients. *Science* **270**, 988–991.
11. Guy, B., *et al.*, & Lecocq, J.P. (1987). HIV F/3′ *orf* encodes a phosphorylated GTP-binding protein resembling an oncogene product. *Nature* **330**, 266–269.
12. Pandori, M.W., *et al.*, & Guatelli, J.C. (1996). Producer-cell modification of human immunodeficiency virus type 1: Nef is a virion protein. *J. Virol.* **70**, 4283–4290.
13. Welker, R., Kottler, H., Kalbitzer, H.R. & Krausslich, H.G. (1996). Human immunodeficiency virus type 1 Nef protein is incorporated into virus particles and specifically cleaved by the viral proteinase. *Virology* **219**, 228–236.
14. Schorr, J., *et al.*, & Kalbitzer, H.R. (1996). Specific cleavage sites of Nef proteins from human immunodeficiency virus types 1 and 2 for the viral proteases. *J. Virol.* **70**, 9051–9054.
15. Freund, J., *et al.*, & Kalbitzer, H.R. (1994). A possible regulation of negative factor (Nef) activity of human immunodeficiency virus type 1 by the viral protease. *Eur. J. Biochem.* **223**, 589–593.

16. Aiken, C., Konner, J., Landau, N.R., Lenburg, M.E. & Trono, D. (1994). Nef induces CD4 endocytosis: requirement for a critical dileucine motif in the membrane-proximal CD4 cytoplasmic domain. *Cell* **76**, 853–864.
17. Salghetti, S., Mariani, R. & Skowronski, J. (1995). Human immunodeficiency virus type 1 Nef and p56lck protein-tyrosine kinase interact with a common element in CD4 cytoplasmic tail. *Proc. Natl. Acad. Sci. USA* **92**, 349–353.
18. Schwartz, O., *et al*., & Danos, O. (1995). Human immunodeficiency virus type 1 Nef induces accumulation of CD4 in early endosomes. *J. Virol.* **69**, 528–533.
19. Schwartz, O., Marechal, V., Le Gall, S., Lemonnier, F. & Heard, J.M. (1996). Endocytosis of major histocompatibility complex class I molecules is induced by the HIV-1 Nef protein. *Nat. Med.* **2**, 338–342.
20. Iafrate, A.J., Bronson, S. & Skowronski, J. (1997). Separable functions of Nef disrupt two aspects of T cell receptor machinery: CD4 expression and CD3 signaling. *EMBO J.* **16**, 673–684.
21. Greenway, A., Azad, A. & McPhee, D. (1995). Human immunodeficiency virus type 1 Nef protein inhibits activation pathways in peripheral blood mononuclear cells and T-cell lines. *J. Virol.* **69**, 1842–1850.
22. Skowronski, J., Parks, D. & Mariani, R. (1993). Altered T cell activation and development in transgenic mice expressing the HIV-1 *nef* gene. *EMBO J.* **12**, 703–713.
23. Chowers, M.Y., *et al*., & Guatelli, J.C. (1994). Optimal infectivity *in vitro* of human immunodeficiency virus type 1 requires an intact *nef* gene. *J. Virol.* **68**, 2906–2914.
24. Miller, M.D., Feinberg, M.B. & Greene, W.C. (1994). The HIV-1 *nef* gene acts as a positive viral infectivity factor. *Trends Microbiol.* **2**, 294–298.
25. Aiken, C. & Trono, D. (1995). Nef stimulates human immunodeficiency virus type 1 proviral DNA synthesis. *J. Virol.* **69**, 5048–5056.
26. Saksela, K., Cheng, G. & Baltimore, D. (1995). Proline-rich (PxxP) motifs in HIV-1 Nef bind to SH3 domains of a subset of Src kinases and are required for the enhanced growth of Nef$^+$ viruses but not for down-regulation of CD4. *EMBO J.* **14**, 484–491.
27. Chowers, M.Y., Pandori, M.W., Spina, C.A., Richman, D.D. & Guatelli, J.C. (1995). The growth advantage conferred by HIV-1 nef is determined at the level of viral DNA formation and is independent of CD4 downregulation. *Virology* **212**, 451–457.
28. Luo, T. & Garcia, J.V. (1996). The association of Nef with a cellular serine/threonine kinase and its enhancement of infectivity are viral isolate dependent. *J. Virol.* **70**, 6493–6496.
29. Sawai, E.T., *et al*., & Cheng-Mayer, C. (1994). Human immunodeficiency virus type 1 Nef associates with a cellular serine kinase in T lymphocytes. *Proc. Natl. Acad. Sci. USA* **91**, 1539–1543.
30. Nunn, M.F. & Marsh, J.W. (1996). Human immunodeficiency virus type 1 Nef associates with a member of the p21-activated kinase family. *J. Virol.* **70**, 6157–6161.
31. Lee, C.H., *et al*., & Saksella, K. (1995). A single amino acid in the SH3 domain of Hck determines its high affinity and specificity in binding to HIV-1 Nef protein. *EMBO J.* **14**, 5006–5015.
32. Collette, Y., *et al*., & Olive, D. (1996). Physical and functional interaction of Nef with Lck. HIV-1 Nef-induced T-cell signaling defects. *J. Biol. Chem.* **271**, 6333–6341.
33. Greenway, A., Azad, A., Mills, J. & McPhee, D. (1996). Human immunodeficiency virus type 1 Nef binds directly to Lck and mitogen-activated protein kinase, inhibiting kinase activity. *J. Virol.* **70**, 6701–6708.
34. Erpel, T. & Courtneidge, S.A. (1995). Src family protein tyrosine kinases and cellular signal transduction pathways. *Curr. Opin. Cell Biol.* **7**, 176–182.
35. DeFranco, A.L. (1995). Transmembrane signaling by antigen receptors of B and T lymphocytes. *Curr. Opin. Cell Biol.* **7**, 163–175.
36. Howe, L.R. & Weiss, A. (1995). Multiple kinases mediate T-cell-receptor signaling. *Trends Biochem. Sci.* **20**, 59–64.
37. Li, B., *et al*., & Kamata, B. (1996). Catalytic activity of the mouse guanine nucleotide exchanger mSOS is activated by Fyn tyrosine kinase and the T-cell antigen receptor in T cells. *Proc. Natl. Acad. Sci. USA* **93**, 1001–1005.
38. Iwashima, M., Irving, B.A., van Oers, N.S., Chan, A.C. & Weiss, A. (1994). Sequential interactions of the TCR with two distinct cytoplasmic tyrosine kinases. *Science* **263**, 1136–1139.
39. Tsygankov, A.Y., Broker, B.M., Fargnoli, J., Ledbetter, J.A. & Bolen, J.B. (1992). Activation of tyrosine kinase p60fyn following T cell antigen receptor cross-linking. *J. Biol. Chem.* **267**, 18259–18262.
40. Pawson, T. (1995). Protein modules and signaling networks. *Nature* **373**, 573–580.
41. Lee, C.H., Saksela, K., Mirza, U.A., Chait, B.T. & Kuriyan, J. (1996). Crystal structure of the conserved core of HIV-1 Nef complexed with a Src family SH3 domain. *Cell* **85**, 931–942.
42. Holtzman, D.A., Cook, W.D. & Dunn, A.R. (1987). Isolation and sequence of a cDNA corresponding to a src-related gene expressed in murine hemopoietic cells. *Proc. Natl. Acad. Sci. USA* **84**, 8325–8329.
43. Bolen, J.B., Rowley, R.B., Spana, C. & Tsygankov, A.Y. (1992). The Src family of tyrosine protein kinases in hemopoietic signal transduction. *FASEB J.* **6**, 3403–3409.
44. Freund, J., *et al*., & Kalbitzer, H.R. (1994). Stability and proteolytic domains of Nef protein from human immunodeficiency virus (HIV) type 1. *Eur. J. Biochem.* **221**, 811–819.
45. Grzesiek, S., *et al*., & Wingfield, P.T. (1996). The solution structure of HIV-1 Nef reveals an unexpected fold and permits delineation of the binding surface for the SH3 domain of Hck tyrosine protein kinase. *Nat. Struct. Biol.* **3**, 340–345.
46. Grzesiek, S., *et al*., & Wingfield, P.T. (1997). Refined solution structure and backbone dynamics of HIV-1 Nef. *Protein Sci.* **6**, 1248–1263.
47. Noble, E.M., Musacchio, A., Saraste, M., Courtneidge, S.A. & Wierenge, R.K. (1993). Crystal structure of the SH3 domain in human Fyn; comparison of the three-dimensional structures of SH3 domains in tyrosine kinases and spectrin. *EMBO J.* **12**, 2617–2624.
48. Fujii, Y., *et al*., & Adachi, A. (1996). Clustered localization of oligomeric Nef protein of human immunodeficiency virus type 1 on the cell surface. *FEBS Lett.* **395**, 257–261.
49. Kienzle, N., Freund, J., Kalbitzer, H.R. & Mueller-Lantzsch, N. (1993). Oligomerization of the Nef protein from human immunodeficiency virus (HIV) type 1. *Eur. J. Biochem.* **214**, 451–457.
50. Musacchio, A., Saraste, M. & Wilmanns, M. (1994). High resolution crystal structures of tyrosine kinase SH3 domains complexed with proline rich peptides. *Nat. Struct. Biol.* **1**, 546–551.
51. Renzoni, D.A., *et al*., & Ladbury, J.E. (1996). Structural and thermodynamic characterization of the interaction of the SH3 domain from Fyn with the proline-rich binding site on the p85 subunit of PI3-kinase. *Biochemistry* **35**, 15646–15653.
52. Morton, C.J., *et al*., & Campbell, I.D. (1996). Solution structure and peptide binding of the SH3 domain from human Fyn. *Structure* **4**, 705–714.
53. Wu, X., *et al*., & Kuriyan, J. (1995). Structural basis for the specific interaction of lysine-containing proline-rich peptides with the N-terminal SH3 domain of c-Crk. *Structure* **3**, 215–226,
54. Weng, Z., *et al*., & Brugge, J.S. (1995). Structure-function analysis of SH3 domains: SH3 binding specificity altered by single amino acid substitutions. *Mol. Cell Biol.* **15**, 5627–5634.
55. Shugars, D.C., *et al*., & Swanstrom, R. (1993). Analysis of human immunodeficiency virus type 1 *nef* gene sequences present *in vivo*. *J. Virol.* **67**, 4639–4650.
56. Ratner, L., *et al*., & Arens, M. (1996). Sequence heterogeneity of Nef transcripts in HIV-1-infected subjects at different stages of disease. *Virology* **223**, 245–250.
57. Janin, J. & Rodier, F. (1995). Protein–protein interaction at crystal contacts. *Proteins* **23**, 580–587.
58. Cho, Y., Gorina, S., Jeffrey, P. & Pavletich, N.P. (1994). Crystal structure of a p53 tumor suppressor–DNA complex: understanding tumorigenic mutations. *Science* **265**, 346–355.
59. Fusaki, N., Matsuda, S., Nishizumi, H., Umemori, H. & Yamamoto, T. (1996). Physical and functional interactions of protein tyrosine kinases, p59fyn and ZAP-70, in T cell signaling. *J. Immunol.* **156**, 1369–1377.
60. Pedrava-Alva, G., Mérida, L.B., Burakoff, S.J. & Rosenstein, Y. (1996). CD43-specific activation of T cells induces association of CD43 to Fyn kinase. *J. Biol. Chem.* **271**, 27564–27568.
61. Atkinson, E.A., *et al*., & Bleackley, R.C. (1996). A physical interaction between the cell death protein Fas and tyrosine kinase p59. *J. Biol. Chem.* **271**, 5968–5971.
62. Qian, D., *et al*., & Weiss, A. (1997). Tyrosine phosphorylation of Pyk2 is selectively regulated by Fyn during TCR signaling. *J. Exp. Med.* **185**, 1253–1259.
63. Moarefi, I., *et al*., & Miller, W.T. (1997). Activation of the Src-family tyrosine kinase Hck by SH3 domain displacement. *Nature* **385**, 650–653.
64. Sicheri, F., Moarefi, I. & Kuriyan, J. (1997). Crystal structure of the Src family tyrosine kinase Hck. *Nature* **385**, 602–609.
65. Kabsch, W. (1993). Automatic processing of rotation diffraction data from crystals of initially unknown symmetry and cell constants. *J. Appl. Cryst.* **26**, 795–800.

66. Collaborative Computing Project, No. 4. (1994). The CCP4 suite: programs for protein crystallography. *Acta Cryst. D* **50**, 760–763.
67. Navaza, J. (1994). AMoRe: an automated package for molecular replacement. *Acta Cryst. A* **50**, 157–163.
68. Brünger, A.T. (1993). *X-PLOR Version 3.1 Manual*. Yale University, New Haven, CT, USA.
69. Jones, T.A., Zou, J.Y., Cowan, S.W. & Kjeldgaard, M. (1993). Improved methods for building protein models in electron density maps and the location of errors in these models. *Acta Cryst. D* **49**, 148–157.
70. Laskowski, R., MacArthur, M., Moss, D. & Thornton, J. (1993). PROCHECK: a program to check the stereochemical quality of protein structures. *J. Appl. Cryst.* **26**, 91–97.
71. Kraulis, P.J. (1991). MOLSCRIPT: a program to produce both detailed and schematic plots of protein structures. *J. Appl. Cryst.* **24**, 946–950.
72. Meritt, E.A. & Murphy, M.E.P. (1994). Raster 3D version 2.0 – a program for photorealistic molecular graphics. *Acta Cryst. D* **50**, 869–873.
73. Nicholls, A., Sharp, K.A. & Honig, B. (1991). Protein folding and association: insights from the interfacial and thermodynamic properties of hydrocarbons. *Proteins* **11**, 281–296.